J|A|C|S
ARTICLES
Published on Web 11/27/2002

Intermolecular Coupling in Nanometric Domains of Light-Harvesting Dendrimer Films Studied by Photoluminescence Near-Field Scanning Optical Microscopy (PL NSOM)

Lynn F. Lee, Alex Adronov,*,† Richard D. Schaller, Jean M. J. Fréchet,* and Richard J. Saykally*

Contribution from the Department of Chemistry, University of California, Berkeley, California 94720

Received September 10, 2002; E-mail: saykally@uclink4.berkeley.edu; frechet@cchem.berkeley.edu; adronov@mcmaster.ca

Abstract: Near-field scanning optical microscopy (NSOM) has been used to investigate the photophysical characteristics of first- to fourth-generation (G1 to G4) light-harvesting dendrimer thin films containing coumarin-343 and coumarin-2 as the core and peripheral chromophores, respectively. Thin film photoluminescence (PL) spectra exhibit a significant red shift in the lower generations (G1, G2, and G3) as compared to their respective solution PL spectra, implying the formation of excimers. Spatially resolved PL NSOM images exhibit pronounced nanoscopic domains in G1, which become more homogeneous in higher generations due to site-isolation of the core chromophore. G4 exhibits complete site-isolation for these light-harvesting dendrimer films.

Introduction

There is much current interest in the study of conjugated organic materials with many applications envisioned in the areas of photonics, sensors, electronics, and solar energy conversion.[1] In the latter context, traditional linear luminescent polymers are not ideal as they can adopt various conformations that depend explicitly on film casting conditions,[2,3] thus making it difficult to achieve the efficient energy transfer required for vectorial transduction of light energy.[4] Recent studies from the Saykally group employing linear[5,6] and nonlinear[7] optical near-field scanning optical microscopy (NSOM) have shown a considerable degree of nanoscopic heterogeneity in the optical properties of conjugated polymer films of poly(2-methoxy-5-(2′-ethylhexyloxy)-1,4-phenylene vinylene) (MEH-PPV), both before and after annealing. Such electronic disorder is known to severely limit device performance.[2,8]

Dendrimers have attracted interest as alternatives to linear polymers for optical devices[9] because, in addition to their highly directional energy transport properties, the three-dimensional dendritic skeletal framework can create a unique core microenvironment by providing an encapsulating cage. This leads to effective site-isolation of the core chromophore that is especially evident in higher generations.[10−13] The globular shape of dendrimers also provides a more rigid framework for the core chromophores, and, although there is a distribution of dendrimer conformations in solution,[14] it is not as pronounced as that of linear polymers due to the restrictive dendritic backbone. Thus, the degree of branching in these macromolecules allows for direct control of intermolecular interactions and photophysical characteristics.

It has been shown that a low degree of site-isolation of the core chromophore affects the photophysical and charge transport properties of a dendrimer at high concentration.[15−17] While many

† Present address: Department of Chemistry, McMaster University, Hamilton, Ontario, Canada L8S 4M1.

(1) For reviews, see: (a) Lovinger, A. J.; Rothberg, L. J. *J. Mater. Res.* **1996**, *11*, 1581−92. (b) Friend, R. H.; Gymer, R. W.; Holmes, A. B.; Burroughes, J. H.; Marks, R. N.; Taliani, C.; Bradley, D. D. C.; Dos Santos, D. A.; Bredas, J. L.; Logdlund, M.; Salaneck, W. R. *Nature* **1999**, *397*, 121−28.
(2) Nguyen, T.-Q.; Martini, I.; Liu J.; Schwartz, B. J. *J. Phys. Chem. B* **2000**, *104*, 237−255.
(3) Nguyen, T.-Q.; Kwong, R. C.; Thompson, M. E.; Schwartz, B. J. *Appl. Phys. Lett.* **2000**, *76*, 2454−56.
(4) Weil, T.; Reuther, E.; Müllen, K. *Angew. Chem., Int. Ed.* **2002**, *41*, 1900−04.
(5) Nguyen, T.-Q.; Schwartz, B. J.; Schaller, R. D.; Johnson, J. C.; Lee, L. F.; Haber, L. H.; Saykally, R. J. *J. Phys. Chem. B* **2001**, *105*, 5153−60.
(6) Schaller, R. D.; Lee, L. F.; Johnson, J. C.; Haber, L. H.; Vieceli, J.; Benjamin, I.; Nguyen, T.-Q.; Schwartz, B. J.; Saykally, R. J. *J. Phys. Chem. B* **2002**, *106*, 9496−9506.
(7) Schaller, R. D.; Snee, P. T.; Johnson, J. C.; Lee, L. F.; Wilson, K. R.; Haber, L. H.; Saykally, R. J.; Nguyen, T.-Q.; Schwartz, B. J. *J. Chem. Phys.* **2002**, *117*, 6688−98.
(8) Nguyen, T.-Q.; Doan, V.; Schwartz, B. J. *J. Chem. Phys.* **1999**, *110*, 4068−78.
(9) For example: (a) Moore, J. S.; Wang, P. W.; Liu, Y. J.; Devadoss, C.; Bharathi, P. *Adv. Mater.* **1996**, *8*, 237−41. (b) Kopelman, R.; Shortreed, M.; Shi, Z.-Y.; Tang, W.; Xu. Z.; Moore, J.; Bar-Haim, A.; Klafter, J. *Phys. Rev. Lett.* **1997**, *78*, 1239−42.
(10) Apperloo, J. J.; Janssen, R. A. J.; Malenfant, P. R. L.; Fréchet, J. M. J. *J. Am. Chem. Soc.* **2001**, *123*, 6916−24.
(11) Lupton, J. M.; Samuel, I. D. W.; Beavington, R.; Frampton, M. J.; Burn, P. L.; Bässler, H. *Phys. Rev. B* **2001**, *63*, 155206−13.
(12) Markham, J. P. J.; Lo, S.-C.; Magennis, S. W.; Burn, P. L.; Samuel, I. D. W. *Appl. Phys. Lett.* **2002**, *80*, 2645−47.
(13) Hecht, S.; Fréchet, J. M. J. *Angew. Chem., Int. Ed.* **2001**, *40*, 75−91.
(14) Neuwahl, F. V. R.; Righini, R.; Adronov, A.; Malenfant, P. R. L.; Fréchet, J. M. J. *J. Phys. Chem.* **2001**, *105*, 1307−12 and references therein.
(15) Lupton, J. M.; Samuel, I. D. W.; Beavington, R.; Burn, P. L.; Bässler, H. *Adv. Mater.* **2001**, *13*, 258−60.
(16) Halim, M.; Pillow, J. N. G.; Samuel, I. D. W.; Burn, P. L. *Adv. Mater.* **1999**, *11*, 371−74.

 10.1021/ja028495a CCC: $25.00

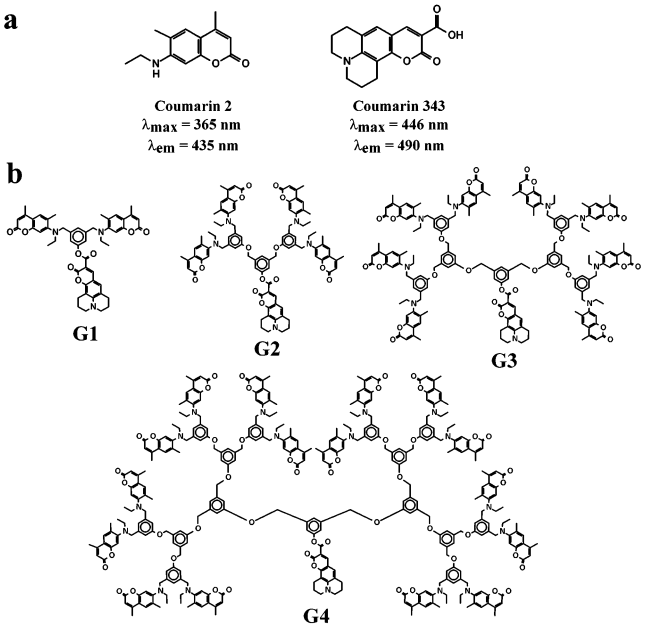

Figure 1. (a) Chemical structures and spectral characteristics of the donor (coumarin 2) and acceptor (coumarin 343) dendrimer components present in a ratio of 2^n:1, respectively, for the *n*th generation. (b) Chemical structures of the fully chromophore-functionalized G1, G2, G3, and G4 dendrimers.

dendrimer studies have been performed in solution,[17,18] investigations of thin films have been more limited.[11,15,16,19] Lupton et al. studied films of stilbene-containing dendrimers in the far-field and found that the dendrimer generation strongly influences the level of interaction between the chromophores, which increases the degree of photoluminescence (PL) quenching and charge.[15,19]

Although the physical properties of dendrimer films are of direct relevance to device fabrication and performance, relatively few NSOM studies, wherein one extracts simultaneous topographic and spectroscopic features on a length scale of ca. 100 nm, have been performed on these materials. Using fluorescence NSOM with circularly polarized excitation, van Hulst et al. were able to distinguish the orientation of discrete Rhodamine B chromophores contained in G3 dendrimers.[20] Here, we use PL NSOM to examine films of dendrimeric species incorporating the laser dyes coumarin 2 (C-2) and coumarin 343 (C-343) (Figure 1) as the peripheral and core chromophores, respectively. Because of their high degree of spectral overlap, energy transfer (ET) between the core and peripheral chromophores is highly efficient and results in amplification of the core emission when the peripheral chromophores are excited.[21,22] Previous studies of these light-harvesting complexes in solution have shown that the ET efficiency is near unity upon excitation of C-2 in the first three generations and decreases to approximately 93% in the fourth generation.[22,23] In the work that follows, we demonstrate that, due to intermolecular interactions, these light-harvesting complexes form spatially heterogeneous films in low generations and become more homogeneous with solution-like PL spectra in higher generations.

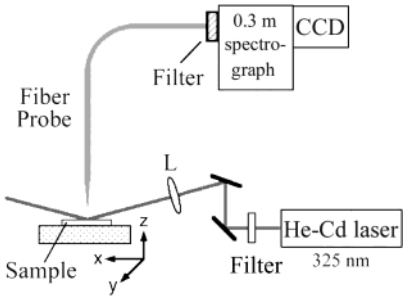

Figure 2. Near-field scanning optical microscope experimental setup: (L) 10 cm focal length plano-convex lens. NSOM measurements were conducted in an oblique collection mode geometry with the angle of incident as ~60° using average power ranging between 1.5 and 5 μW; the diameter of the laser spot is ca. 250 μm. Neutral density filters and a 442 nm notch filter are placed in front of the He−Cd laser. The 0.3 m spectrograph, long-pass 500 filter, and CCD used to acquire the spectra were replaced with a PMT (Hamamatsu, R3896) and a long-pass 600 nm filter for SRPL imaging.

Experimental Section

The synthetic routes to G1 through G4 have been discussed elsewhere.[23] The chemical structures of the chromophores and dendrimers studied here are shown in Figure 1. Dendrimer properties are studied as a function of generation in films ca. 200 nm thick measured by NSOM. The films were spin-cast under ambient conditions from dichloromethane with solution concentrations of typically 40 mg/mL on acid-cleaned, Al-plated glass substrates at 1500 rpm for several minutes to ensure complete evaporation of the solvent.

Far-field absorption and PL spectra of solutions of all generations were performed on a Hewlett-Packard 8453 UV−vis spectrometer and a Spex 1681 fluorimeter, respectively, in 1 cm quartz cuvettes, using dichloromethane or toluene as solvents. An excitation wavelength of 325 nm produced by a CW He−Cd laser (Melles Griot) was used for all far- and near-field optical measurements.

Near-field spatially resolved photoluminescence (SRPL) measurements and topographical images of the dendrimer films were obtained using a commercial NSOM system (TMmicroscopes, Lumina) equipped with a noncontact (~5−10 nm separation), tuning fork-based shear-force feedback mechanism. Figure 2 shows a schematic of the experimental configuration. The laser beam was focused with a 10 cm focal length lens to produce an ca. 250 μm diameter spot on the sample, and average power ranged between 1.5 and 5 μW (the generations had different optical densities at the excitation wavelength, so the incident laser power was changed accordingly). Optical signals were collected with a chemically-etched, uncoated SiO_2 optical fiber, ca. 50 nm tip diameter,[24] and were directed to either a CCD camera to produce SRPL spectra or a preamplified photomultiplier for NSOM imaging. To obtain SRPL spectra, collected PL signals were directed through a 500 nm long-pass filter, dispersed with a 150 gr/mm grating and a 0.3 m spectrograph, and detected with a CCD camera. For imaging studies, a R3896 Hamamatsu photomultiplier tube was used with a long-pass 600 nm filter and a SRS SR560 preamplifier. All presented images consist of 200 × 200 pixel arrays. Measurements were conducted under a nitrogen atmosphere to minimize photooxidation.

Topographical and optical signals were obtained simultaneously for comparison. The forward and reverse scanning motions of the sample were collected to produce separate images as a check of reproducibility. As shown in Figure 2, near-field measurements were conducted in an

(17) Pollak, K. W.; Leon, J. W.; Fréchet, J. M. J.; Maskus, M.; Abruna, H. D. *Chem. Mater.* **1998**, *10*, 30−38.
(18) Adronov, A.; Fréchet, J. M. J. *Chem. Commun.* **2000**, *18*, 1701−10.
(19) Lupton, J. M.; Samuel, I. D. W.; Beavington, R.; Burn, P. L.; Bässler, H. *Synth. Met.* **2001**, *116*, 357−62.
(20) van Hulst, N. F.; Veerman, J.-A.; Garcia-Parajo, M. F.; Kuipers, L. *J. Chem. Phys.* **2000**, *112*, 7799−7810.
(21) Gilat, S. L.; Adronov, A.; Fréchet, J. M. J. *Angew. Chem., Int. Ed.* **1999**, *18*, 1422−27.
(22) Gilat, S. L.; Adronov, A.; Fréchet, J. M. J. *J. Org. Chem.* **1999**, *64*, 7474−84.
(23) Adronov, A.; Gilat, S. L.; Fréchet, J. M. J.; Ohta, K.; Neuwahl, F. V. R.; Fleming, G. R. *J. Am. Chem. Soc.* **2000**, *122*, 1175−85.
(24) Hoffman, P.; Butoit, B.; Salathe, R.-P. *Ultramicroscopy* **1995**, *61*, 165−70.

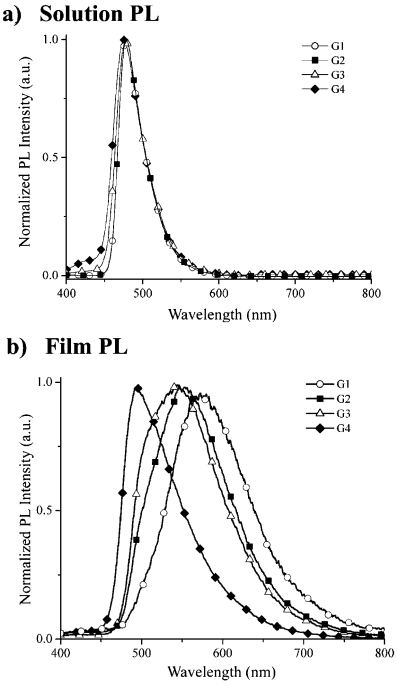

Figure 3. Far-field photoluminescence spectra of G1−G4. (a) Solution PL spectra of G1 (○), G2 (■), G3 (△), and G4 (◆) in dichloromethane (∼10 μM) with 325 nm excitation wavelength. (b) Thin film PL spectra of G1, G2, G3, and G4. All samples were excited with the 325 nm line of a He−Cd laser, and emission was dispersed with a 0.3 m spectrograph and 150 gr/mm grating and detected with a CCD camera. λ_{max} and the fwhm of each generation are summarized in Table 1. The film PL spectra are red-shifted relative to the solution PL, with G1 having the largest shift (greater than 100 nm) and G4 having the smallest (∼10 nm). The shape of the PL spectra also changes with generation. Existence of a red tail can be observed with the lower generations.

oblique collection mode geometry with the angle of incidence being ∼60°. To maintain a constant tip/field geometry, the NSOM probe and excitation laser spot remained fixed during all measurements; spatial imaging was performed by scanning the sample stage in the *x* and *y* as well as the *z* (feedback) directions. After the topography of a region was measured, the near-field probe was directed via computer control to different positions of the sample, and the SRPL spectra were acquired at each indicated point. The experimentally observed lateral optical resolution, which is obtained by a line trace of the optical image and determined by the fwhm of the sharpest reproducible peak in the trace, for G1 is ca. 60 nm full width at half-maximum (fwhm).

Results and Discussion

Far-field PL spectra of successive dendrimer generations are shown in Figure 3a for dichloromethane solutions (∼10 μM). It is observed that their spectra are all very similar, showing only a slight blue shift of ∼5 nm to higher energy as the generation number is increased. However, in films, a large (80 nm) blue shift occurs going from G1 to G4 and the shape of the PL spectra changes (Figure 3b). Film spectra are also dramatically red-shifted relative to solution spectra. In solution, the emission maximum of G1 is at ∼480 nm, while in film its PL maximum is nearly 600 nm. Table 1 summarizes the central emission wavelength and the fwhm of G1 to G4 far-field film PL spectra.

Both solution and film far-field PL spectra (Figure 3) show evidence that the dendritic backbone structure becomes a more important factor in establishing the environment polarity with higher generations. The relative polarity of the solvent to the dendron backbone affects the shift of the PL spectra of the different generations; with higher generations, the core is well encapsulated within the dendron structure, and the polarity of its local environment is mainly established by the backbone. With a more polar solvent, such as dichloromethane ($\epsilon = 8.93$),[25] a progressive blue shift is observed at higher generations as the local core environment becomes less polar (Figure 3a). Conversely, a less polar solvent, such as toluene ($\epsilon = 2.38$)[25] (data not shown), shows the opposite trend of increasing red shift with higher generations, although the integrity of the spectral shape is retained in both solvents. Adronov et al. have also observed similar trends using toluene, acetonitrile, and methanol as solvents.[23]

Table 1. Values of the Central Emission Wavelength and fwhm of the Dendrimer Film Far-Field Fluorescence Spectra

generation	central wavelength (nm)	fwhm (cm^{-1})
G1	573	3273
G2	547	3765
G3	543	3926
G4	495	2952

For the spin-cast thin films, we observe a progressive blue shift with higher generations. We suggest that the polarity of the local environment in films is determined mainly by the intermolecular proximity of the core chromophore to its neighboring chromophores, be they core or peripheral, and by the dendritic structure. In lower generations, where the core chromophore is more exposed and accessible, interaction with neighboring chromophores produces a relatively polar local environment, whereas with higher generations, the local polarity of the core decreases.

It is found that for decreasing generation number, a low energy band emerges in the SRPL that is most prominent in the G1 film. This is supported by the observation that the blue portion of the PL curve becomes significant at higher generations and is especially evident in G3 (Figure 3). The G3 spectrum has the largest fwhm (3926 cm^{-1}), and the fwhm decreases going from G3 to G1 (3273 cm^{-1}), while G4 has the narrowest width of 2952 cm^{-1} (Table 1). In addition, the maximum PL (energy) shift is the greatest between G3 and G4 (1786 cm^{-1}). High concentration conditions in films thus appear to have greater effects on lower generation PL, while the photophysical properties of higher generation films resemble those observed in dilute solutions. Lupton et al.[19] have performed similar far-field dendrimers film studies and report similar trends of higher generation blue-shifting spectra, which are also evident in the electroluminescence (EL) spectra.[12,16]

Figures 4 and 5 show PL NSOM images, their corresponding topographic profiles, and the SRPL spectra of different areas of the G1 and G4 films, respectively. Figure 4 shows a 5 × 5 μm scanned area for G1, while a 10 × 10 μm scanned area is presented in Figure 5 for G4. With successively higher generations, the film topographies become smoother. The topographical bumps are believed to be formed by the physical agglomeration of the dendrimers, in which the degree of physical agglomeration is possibly due to film processing procedures.[2,3] SRPL spectra were taken at numerous locations on the films using a long-

(25) *CRC Handbook of Chemistry and Physics*, 81st ed.; CRC Press LLC: Florida, 2000.

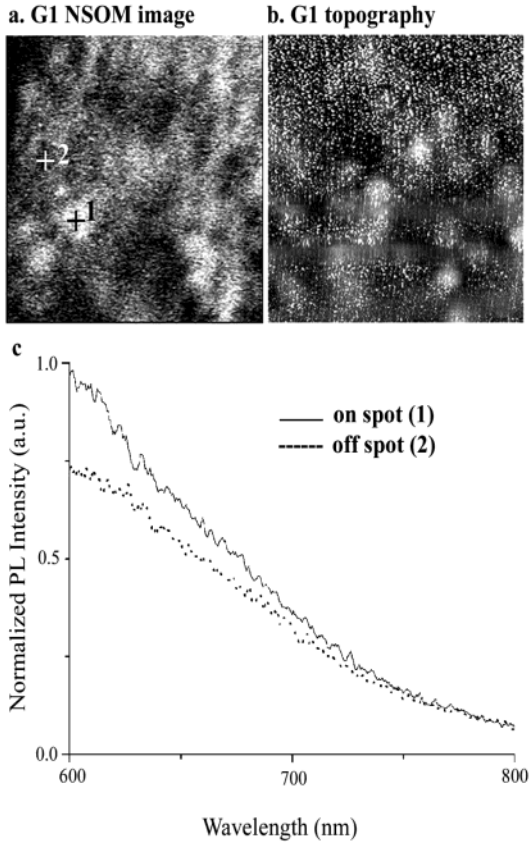

Figure 4. NSOM image and corresponding topographic profile of G1 in a 5 × 5 μm area of the dendrimer thin film. The normalized SRPL spectra are representative of different areas on the film. (a) NSOM image of G1 film. The optical resolution is measured to be ~60 nm fwhm, obtained by a line trace of the optical image. The resolution is determined by the fwhm of the sharpest peak in the line trace. (b) Topography of the G1 film. The maximum height is 65 nm. (c) SRPL of distinct features in the film, as labeled on the NSOM image. "On spot" and "off spot" here refer to the bright spots in the NSOM image. The average bright domain diameter size for the G1 film is measured to be ca. 350 nm.

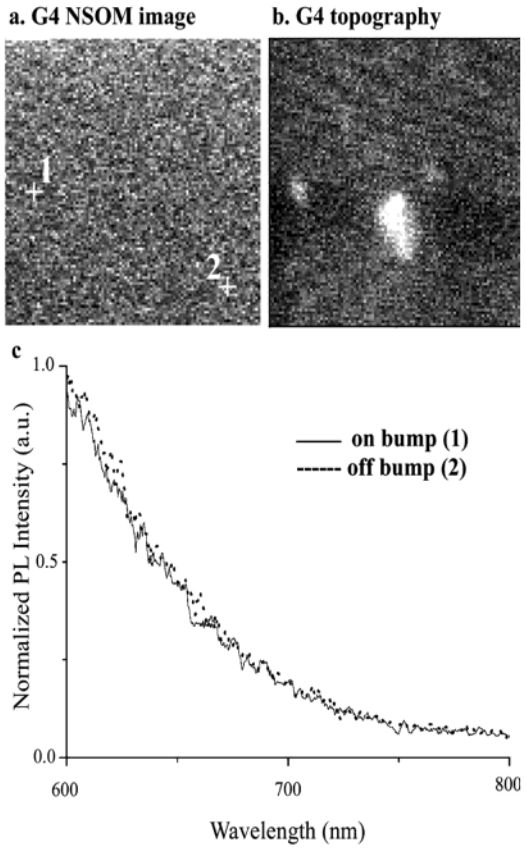

Figure 5. NSOM image and corresponding topographic profile of G4 in a 10 × 10 μm area of the dendrimer thin film. The normalized SRPL spectra are representative of different areas on the film. (a) NSOM image of the G4 film. (b) Topography of the G4 film. The maximum height is 27 nm. (c) SRPL of various spots in the film. Because no contrast is observed in the NSOM image, the "on bump" and "off bump" here refer to topography features.

pass 500 nm filter. Figures 4c and 5c show the SRPL spectra taken at the indicated positions and are representative of the PL trends.

In Figure 4a, the G1 film exhibits numerous domains (average size ca. 350 nm) in the NSOM image, which only occasionally correspond to the topography. Because the red shift is indicative of increased delocalization of the electronic wave function[2] in the dendrimer films, the PL NSOM image was taken with a long-pass 600 nm filter; therefore, the domains represent the intensity variations of the red tail shown in Figure 4c. The bright regions in the NSOM image correspond to high intensity of the red tail, while intermediate regions show different degrees of intensity. Off of the bright NSOM domains, there is little or no evidence of the 600 nm feature, similar to what is observed in G4 (Figure 5c). As the generations increase from G1 to G2 and G3 (data not shown), there is less variation, and, correspondingly, fewer bright domains are seen in the respective NSOM images. Figure 6 summarizes the average percentage domain coverage in the NSOM images per unit area of the film. An exponential decrease in coverage is shown between the four generations: approximately 19% coverage is observed in G1, decreasing to 5% and 0.5% for G2 and G3, respectively, while G4 shows no domains (Figure 5a). G4 does not exhibit any variations in the intensity of the 600 tail as shown in Figure 5c

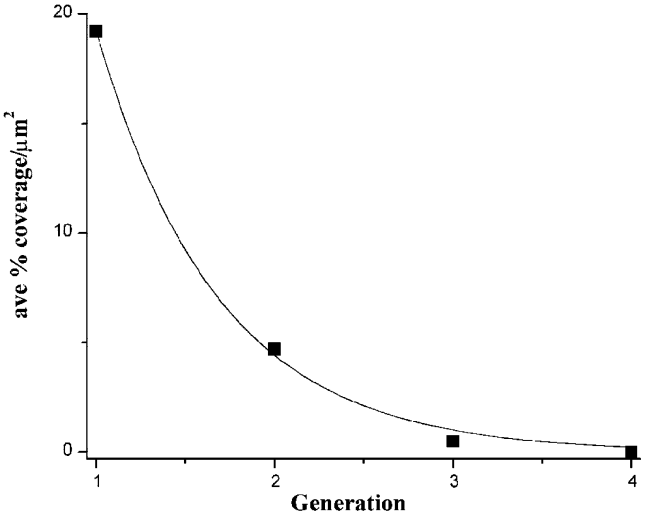

Figure 6. The average percentages of domains in the NSOM image per square area of G1 through G4 (■). The percentages were statistically obtained from the results of approximately 10 scans. The fitted curve shows an exponential decay.

and, correspondingly, produces an optically homogeneous film in emission. Spectra taken of the G4 film using a LP 335 filter also did not show variations in the red tail, indicating that the red feature in G4 did not shift to higher energy like the PL maximum.

van Hulst et al. also observed NSOM domains that did not correspond to topographical features and concluded that these are due to Rhodamine B chromophores that were not attached to the dendritic structure.[20] In our study, the intensity variations of the red feature in the SRPL indicate that the NSOM domains are not due to unreacted C-343 molecules. Instead, we suggest that the red feature in the PL is indicative of intermolecular electronic interaction,[26] and the absence of a corresponding component in the ground state absorption (not shown) suggests that the red component is most likely due to excimer formation.[19] For high generations, the core is shielded within the dendron cage, and the degree of intermolecular interaction is low, as shown in Figure 6 where G4 exhibits complete site-isolation for these light-harvesting dendrimers. Higher generations are likely to exhibit results similar to those of G4.

Previous studies have also shown the existence of the red feature in dendrimer films. Fréchet and co-workers, as well as work performed by Samuel and Burn, have independently concluded that the observed red feature is due to intermolecular interactions in the films; in particular, they conclude that it is the result of excimer formation in the early generations.[11,19,26,27] The reduced intermolecular interactions with higher generations are also implicated in the transport characteristics of single layer LEDs, where the requisite operating electric field increases as the branching increases.[11,19,27] In solution studies of linear polymers with C-2 and C-343 chromophores attached in appropriate concentration ratios to match those found in the respective dendrimers, Fréchet and co-workers show evidence that the C-343 chromophores have a tendency to interact.[26] At higher concentrations, where interactions between different polymer strands become more prominent, they observed excimer formation between C-343 chromophores, which diminished the fluorescence quantum yield, while interactions between multiple C-2 chromophores or between C-2 and C-343 chromophores are not favored. On the basis of these studies, we believe excimer formation in films of these light-harvesting dendrimers is primarily due to the core−core interactions. Additional studies using nonlinear NSOM techniques may further elucidate the nature of these intermolecular interactions, as in our recent investigations of conjugated linear polymers.[28]

Finally, to see if domains exhibiting increased red emission in the dendrimer films were mathematically correlated at distances greater than that of the individual domains, as would be indicated by a $g(r)$ greater than 1 at long distances, we digitally filtered the PL NSOM images by comparing the value of each individual pixel to a threshold level and performed radial distribution function (RDF)[29] analysis on the resulting image as described in ref 7. Pixels above the threshold value with more than three nearest neighbor pixels also above the threshold (to account for instrument spatial resolution) were given a value of 1. Those that did not meet the threshold value or nearest neighbor criteria were given a value of zero. Films of all four dendrimer generations were analyzed, and a two-dimensional RDF of the digitally filtered image is shown (Figure 7) for the G1 film in Figure 4, as G1 would be expected to exhibit the most structure. For a large range of arbitrary threshold values, the RDFs of all generations showed little structure, indicating that interchromophore domains are not correlated beyond the domain size (ca. 350 nm for G1) and are not highly ordered in the films. This lack of correlation between dendrimer domains is expected and indicates that the formation of an interchromophore domain does not affect the formation of others. Unlike the case in linear polymer systems, such as MEH-PPV whose ground-state aggregation is correlated,[7] the defined, globular shape of the dendrimer causes the macromolecule to be more rigid, which does not allow as many possible conformations as compared to the linear polymers. In addition, its more compact structure does not contain loose ends that can act as individual aggregation sites.

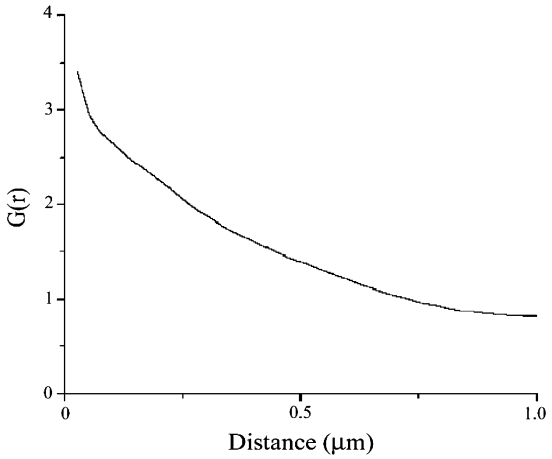

Figure 7. Calculated radial distribution function for G1 film (Figure 4). The RDF shows little structure beyond the domain size, indicating that the interchromophore domains are uncorrelated.

Conclusions

We have demonstrated that the photophysical properties of dendrimer thin films are dependent upon the dendrimer generation. PL NSOM imaging of the red edge of the emission shows the films to become more spatially homogeneous in terms of core chromophore isolation as the generation number increases. For this C-2, C-343 dendrimer system, essentially complete site-isolation is achieved by the fourth generation.

Acknowledgment. This work was supported by the Experimental Physical Chemistry Division of the National Science Foundation, the Air Force Office of Scientific Research, and the U.S. Department of Energy (LBNL-MSD). The authors thank Delia Milliron and Deborah Aruguete for assistance in preparation of the thin films and Preston Snee for assistance with the RDF calculations.

JA028495A

(26) Adronov, A.; Robello, D. R.; Fréchet, J. M. J. *J. Polym. Sci., Part A* **2001**, *39*, 1366−73.
(27) Lupton, J. M.; Samuel, I. D. W.; Beavington, R.; Burn, P. L.; Bässler, H. *Synth. Met.* **2001**, *121*, 1703−04.
(28) Schaller, R. D.; Johnson, J. C.; Wilson, K. R.; Lee, L. F.; Haber, L. H.; Saykally, R. J. *J. Phys. Chem. B* **2002**, *106*, 5143−54.
(29) Chandler, D. *Introduction to Modern Statistical Mechanics*; Oxford University Press: New York, 1987.